Ocean Engineering 35 (2008) 1015–1028

Contents lists available at ScienceDirect

Ocean Engineering

journal homepage: www.elsevier.com/locate/oceaneng

2D Wave setup behind submerged breakwaters

M. Calabrese [a], D. Vicinanza [b,*], M. Buccino [a]

[a] Department of Hydraulic and Environmental Engineering, University of Naples "Federico II", Via Claudio 21, 80125 Naples, Italy
[b] Department of Civil Engineering, Second University of Naples, Via Roma 29, 81031 Aversa (Caserta), Italy

ARTICLE INFO

Article history:
Received 19 April 2007
Accepted 3 March 2008
Available online 13 March 2008

Keywords:
Submerged breakwaters
Hydraulic response
Large wave flume
Small wave flume
Wave setup

ABSTRACT

In addition to reducing the incoming wave energy, submerged breakwaters also cause a setup of the sea level in the protected area, which is relevant to the whole shadow zone circulation, including alongshore currents and seaward flows through the gaps. This study examines such a leading hydraulic parameter under the simplified hypothesis of 2D motion and presents a prediction model that has been validated by a wide ensemble of experimental data. Starting from an approach originally proposed by Dalrymple and Dean [(1971). Piling-up behind low and submerged permeable breakwaters. Discussion note on Diskin et al. (1970). Journal of Waterways and Harbors Division WW2, 423–427], the model splits the rise of the mean water level into two contributions: one is due to the momentum flux release forced by wave breaking on the structure, and the other is associated with the mass transport process. For the first time, the case of random wave trains has been explicitly considered.

1. Introduction

In situations where landscape safeguarding is a major concern (Italian coasts are an important example), submerged breakwaters are frequently employed as shore-protection measures, often in conjunction with beach-nourishment. Despite the fact that they have long been employed, with different design philosophies, either in Europe or in the United States or in Japan, substantial uncertainties still remain on the predictability of shoreline response to their placement; in fact a limited or deleterious effect of structures on coastline equilibrium and nearshore profile has been often documented (Seji et al., 1987; Ranasinghe and Turner, 2006).

For this reason, a number of research projects have recently focused on how the structures affect the shadow-zone hydrodynamics; among them the EU projects *DELOS* (Lamberti, 2005), which has also investigated the compatibility of breakwaters with marine environment, and *Low Crested and Submerged Breakwaters in Presence of Broken Waves* (Calabrese et al., 2002), which has analyzed the hydraulic response of structures under extreme climatic conditions, must be mentioned. Following the suggestions coming from both field measurements and numerical simulations, a substantial amount of work has been directed to wave transmission across the breakwater, since it has been recognized as one of the fundamental mechanisms governing the long-term evolution of the protected beach. Regarding this matter, research outcomes seem quite encouraging, seeing that a number of reliable design tools have been proposed, including empirical formulae (van der Meer et al., 2005), neural networks (Panizzo et al., 2003) and conceptual equations (Buccino and Calabrese, 2007). Nevertheless, other leading factors deserve to be researched in depth.

In analyzing the emblematic case of Palm Beach, Florida, where nearly 82,000 m^3 of sand were lost (over three years) after the placement of an experimental proprietary submerged breakwater of 1260 m length, Dean et al. (1997) reasoned that a key role in the erosive process was played by longshore currents that transported sand from the landward of breakwater towards the heads. These transverse flows were most likely driven by a setup of the mean sea level behind the structure, caused by both wave momentum release and mass transport processes associated with wave overpassing. Just the alongshore variation of this setup evidently allowed the water to be directed parallel to the breakwater and then offshore.

Hence, we recognize the structure-induced variation of the mean water level to be a very important flow parameter for engineering purposes, also considering its effect on segmented systems, where any passages through the barriers have a seaward current that may jeopardize the safety of swimmers (Bellotti, 2004). Nevertheless, the phenomenon has been little investigated so far, although some attention has been drawn to the analogous case of coral reefs (see for instance Gourlay, 1996). Moreover, in the past no research addressed the case of random waves, though it is receiving now a growing attention, especially among the Italian researchers (e.g. Cappietti et al., 2006).

This study focuses on the quantitative prediction of wave setup behind submerged breakwaters with respect to the idealized case

* Corresponding author. Tel.: +39 3385059599; fax: +39 0815037370.
E-mail addresses: calabres@unina.it (M. Calabrese), diegovic@unina.it (D. Vicinanza), buccino@unina.it (M. Buccino).

0029-8018/$ - see front matter
doi:10.1016/j.oceaneng.2008.03.005

Nomenclature

A_c	area of the breakwater cross-section
A_r	area of the surface roller in the vertical plane
B_0	wave peakedness parameter
B	breakwater crest width
B_{eq}	breakwater equivalent crest width A_c/h_c
c	phase speed
$D_{(50)a,c}$	nominal rock diameter $(M_{(50)a,c}/\rho_r)^{1/3}$. The suffixes "a" and "c" stand for armour and core, respectively
E	wave energy
f	friction parameter
g	gravity acceleration
h_I	still water depth offshore the barrier
h_{II}	still water depth inshore the barrier
h_b	still water depth at incipient breaking
h_c	breakwater height
h_P	height of the impermeable part of the breakwater
H_0	deep water regular wave height
H_b	wave height at incipient breaking
H_i	incident regular wave height
H_R	reflected regular wave height
H_t	transmitted regular wave height
$H_{(rms)i,R,t}$	energetically equivalent wave height $\sqrt{8m_0}$. The suffixes "i", "R" and "t" stand for incident, reflected and transmitted, respectively
$H_{(\mu)i,R,t}$	mean wave height $\sqrt{2\pi \cdot m_0}$. The suffixes "i", "R" and "t" stand for incident, reflected and transmitted, respectively
k_I	wave number offshore the barrier
k_{II}	wave number inshore the barrier
K_R	reflection coefficient, H_R/H_i *or* $\sqrt{m_{0R}/m_{0i}}$
K_t	transmission coefficient, H_t/H_i *or* $\sqrt{m_{0t}/m_{0i}}$
L_0	regular deep water wavelength
L	regular wavelength
L_p	peak wavelength
$m_{(0)i,R,t}$	zero order moment of power spectrum; the suffixes "i", "R" and "t" stand for incident, reflected and transmitted, respectively
M_{50}	50% value of rock mass distribution curve
q_{in}	volume flux entering the protected area
R	hydraulic radius
R_c	crest freeboard; it is negative when the crest is submerged
s_0	fictional wave steepness H_i/L_0
S_{JJ}	JJ component of the radiation stress tensor
T	regular wave period
T_p	peak wave period
U_R	Ursell number
V	alongshore velocity at breakwater head
α,β	correction factors
δ	total wave setup behind the barrier
δ'	difference between mean water levels behind and in front of the barrier
δ_c	continuity wave setup behind the barrier
δ_{mf}	momentum flux wave setup behind the barrier
ρ_r	rock density
ρ_w	water density

of 2D motion. As a consequence of alongshore flow being impeded, an upper limit (or "potential" value) is of course obtained, which, however, may be of significance for engineering applications for several reasons. First 2D wave setup might be included within simplified circulation models, which aid engineers at a preliminary stage of the design process (examples are given at the end of the article); for another it may serve as a reference for open flow situations, where, as argued by Lamberti et al. (2007), any effects due to the real 3D motion could be separately calculated and then subtracted from the potential rise of the mean sea level (e.g. Eq. (13.88) of the Lamberti et al. (2007) paper). Finally, in the context of mathematical modelling, 2D wave setup gives a boundary value of the mean water level for zones of computing domain, such as along a cross-shore symmetry axis (Dalrymple, 1978), in which the motion is expected to be nearly planar.

The article is organized as follows: first, a detailed review of previous research is given to provide the reader with the entire spectrum of published predictive equations. Then, after a critical analysis of literature, the central part of the work deals with an alternative model based on the balance of momentum between two fixed vertical planes enclosing the structure cross-section. Originally the model has been developed within *Low Crested and Submerged Breakwaters in Presence of Broken Waves* (Calabrese et al. 2003, 2005), but it has never been expounded properly. In the following, the case of a regular train of waves is considered first: all the hypotheses are widely discussed and predictive power of the new method is compared with that of the other equations; for this purpose a good deal of new experiments carried out at the University of Naples "Federico II" have been employed. In addition the model has been modified to make it more consistent from a physical point of view; modifications include accounting of wave reflection and a better modelling of wave breaking occurrence onto the breakwaters. As a further matter of novelty, the role of structure permeability is investigated.

In the concluding sections adaptation of the model to random seas is addressed and its possible application to both practical engineering and research fields is discussed.

2. Review of existing models

To the knowledge of the authors, the setup of the sea level past a submerged breakwater was first described in Homma and Sokou (1959) and Homma and Hoikawa (1961). However, only a qualitative view of the phenomenon was provided there, without any analysis on parameters that control its magnitude.

At the end of the 1960s, Longuet-Higgins (1967) developed an analytical solution by considering the time-averaged flux of vertical momentum into a column of water included between the still water level and the free surface. Under the hypotheses of small amplitude waves and irrotational motion, which excludes any energy loss, either by breaking or friction or other means, the authors arrived at the following expression, which returns the difference of mean water levels, δ', between two regions of uniform depth shoreward and seaward a submerged breakwater (Fig. 1):

$$\delta' = \frac{H_i^2(1+K_R^2)k_I}{8\,\sinh(2k_I h_I)} - \frac{H_i^2 K_t^2 k_{II}}{8\,\sinh(2k_{II} h_{II})}. \tag{1}$$

In Eq. (1) H_i is the incident wave height, K_R is the reflection coefficient (reflected to incident wave height ratio) and K_t is the transmission coefficient (transmitted to incident wave height ratio); $k_{I,II}$ and $h_{I,II}$, respectively, represent the wave number and the water depth offshore (subscript I) and inshore (subscript II) the structures. It is easy to realize that Eq. (1) represents the difference between the mean water levels at each of the uniform

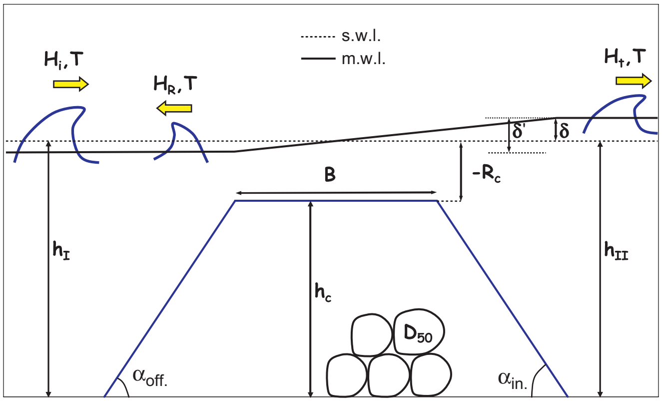

Fig. 1. Definition sketch of breakwater cross-section.

depth Regions I and II, calculated by the second order Stokes wave theory (Longuet-Higgins and Stewart, 1962). Despite the irrotational hypothesis being scarcely verified in practice, the formula has the advantage of clearly highlighting the role of both reflection and transmission processes; more reflection enhances setup, whereas wave transmission acts in the opposite sense.

Longuet-Higgins theory has been experimentally evaluated by Dick (1968), who performed regular wave tests on an impermeable rectangular breakwater model. The author found Eq. (1) to greatly underestimate the experimental data.

Some years later, results of an extensive experimental research conducted at the Technion Israel Institute of Technology of Haifa (Israel) were published by Diskin et al. (1970). The authors carried out nearly 190 2D regular wave experiments on homogeneous breakwater models, with fixed side slopes ($\tan\alpha_{\text{off.}} = \tan\alpha_{\text{in.}} = 1{:}3$), rock size ($D_{50}\cong 2.5$ cm) and crown width ($B = 10$ cm); wave height and period were varied within reasonably wide ranges and both underwater and protruding configurations were considered. It was found out that experimental values of wave setup past the breakwaters, δ, could be approximated, on an average, by the following empirical relationship:

$$\frac{\delta}{H_0} = 0.60\,\exp\left[-\left(0.70 - \frac{R_c}{H_0}\right)^2\right], \qquad (2)$$

where H_0 is the deep water wave height, which the authors calculated as the ratio between the measured incident one, H_i, and the linear shoaling coefficient. We see that in the equation above, that holds for both submerged and emerged structures, the rise of the sea level is related to the crest freeboard by means of a bell-shaped Gaussian curve. The maximum of the curve is at $R_c/H_0 = 0.7$; that is to say, when the water level is just below the top of the breakwater. For water levels above and below this value, δ decreases and tends to zero. Eq. (2) should be used within the ranges:

$$-2.0 < \frac{R_c}{H_0} < 1.5, \qquad (3)$$

$$0.10 < \frac{h_I}{H_0} < 0.83. \qquad (4)$$

It is worth noting that wave period does not appear in the formula, although the authors recognized it to play some role in the wave setup development. As expected, neither crown width, nor armour unit diameter (and consequently permeability), nor side slopes are included in the predictive equation.

Two very interesting discussion notes followed the Diskin et al. (1970) paper: one by Gourlay (1971) and the other, of a more quantitative nature, by Dalrymple and Dean (1971).

Dalrymple and Dean (1971) commented that the scatter between the data of Diskin et al. (1970) and Eq. (2) could be explained by the authors not having included in the formula either the transmission or the reflection coefficients, the role of which had been previously pointed out by Longuet-Higgins (1967). Furthermore, they proposed a predictive procedure that might be considered as the starting point of the conceptual method we are going to present and discuss in the next sections.

The procedure (for submerged breakwaters only) assumes the wave setup to be forced partly by the release of momentum flux due to wave breaking, and partly by the need for a return current to occur in order to compensate for the flux of water mass entering the protected area over the crest of the structure. δ is then thought as the sum of two contributions:

$$\delta = \delta_{mf} + \delta_c. \qquad (5)$$

The "momentum flux" contribution, δ_{mf}, has been treated the same as the wave setup at a beach. Starting from the conservation of horizontal momentum (Longuet-Higgins and Stewart, 1962), under the shallow water hypothesis and assuming the wave height to depth ratio to be constant, the authors obtained

$$\delta_{mf} = 0.15(h_b + R_c), \qquad (6)$$

where h_b indicates the water depth at incipient breaking, which can be estimated by the solitary wave breaking criterion $h_b = 1.28H_i$.

The "continuity" setup, δ_c, is calculated by imposing the net mass influx over the breakwater to be returned offshore over and through the barrier:

$$q_{in} = q_{over} + q_{through}. \qquad (7)$$

As far as the incoming water mass, q_{in}, is concerned, the authors supposed it to be a fraction of the incident waves Stokes drift:

$$q_{in} = \beta\,\frac{E}{\rho_w c}, \qquad (8)$$

where ρ_w is the water density, $E = \frac{1}{8}\rho_w g H_i^2$ is the incident wave energy, g is the gravity acceleration and c is the phase speed of the incident (linear) waves, calculated at the offshore toe of the barrier, h_I. The key factor β, less than unity, depends on the time interval, over a wave period, in which the water surface exceeds the breakwater crest. Using the small amplitude wave theory, Dalrymple and Dean (1971) obtained:

$$\beta = \frac{1}{\pi}\left\{\cos^{-1}(2\upsilon) + \frac{1}{2}\sin[2\cos^{-1}(2\upsilon)]\right\}, \qquad (9)$$

where

$$\upsilon = \frac{(R_c - (\delta_{mf} + \delta_c)/2)}{H_i} \qquad (10)$$

is the "effective" relative crest freeboard, including the setup height. Obviously $\beta = 1$ for $\upsilon \leqslant -\frac{1}{2}$, as in this case the crest of the breakwater lies under the wave trough. Although a hypothetical Darcy type formula was suggested for calculating $q_{through}$, the authors observed, from a comparison with Diskin et al. (1970) data, that reasonable predictions of the total setup could be obtained by a simplified mass balance, in which q_{in} was entirely equated to the backflow over the structure. The latter has been estimated according to the expression reported below:

$$q_{over} = \sqrt{2g\delta_c}\left(\frac{\delta_{mf} + \delta_c}{2} - R_c\right), \qquad (11)$$

which is based on the hypothesis that the hydraulic head δ_c is fully converted into kinetic energy. Clearly, the mass balance, Eq. (7), must be iteratively solved for δ_c to obtain the total setup δ.

More recently, Loveless et al. (1998), in the frame of a research program funded by the UK Ministry of Agriculture Fisheries and Foods, carried out at the University of Bristol a substantial number of experiments on submerged and low-crested breakwaters with homogeneous cross-sections. Based on regular wave tests, the authors proposed the following formula, which is valid for both positive and negative clearances:

$$\frac{\delta}{B}=\frac{(H_{\mathrm{i}}L/\pi h_{\mathrm{I}}T)^2}{gD_{50}}1.23\ \exp\left[-20\left(\frac{R_{\mathrm{c}}}{h_{\mathrm{c}}}\right)^2\right], \tag{12}$$

where besides the symbols already introduced, L is the local incident wavelength, T is the incident wave period and h_{c} is the structure height.

The Loveless et al. (1998) idea is that the breakwater cross-section functions like a weir and the wave height serves as hydraulic head; owing to the wave damping, the head at the inshore side of the barrier is smaller when compared with the one at the offshore side, and the water discharged into the shadow zone during the first half period is not balanced by an equal outflow during the second half period. This misbalance is also amplified by the circumstance that the small head constraints the return current to take place (partly) through the barrier, increasing the backflow resistances. Eventually, the mass flux difference allows the water to "pile up" shoreward the barrier, until an equilibrium state is reached.

Consistent with the above statements, Eq. (12) models δ as the hydraulic head required to drive back by seepage, the volume flux discharged by the incident waves over a half-period. For linear waves this flow rate just equals

$$Q_W=\frac{2}{T}\int_{-T/4}^{+T/4}\mathrm{d}t\int_{-d_{\mathrm{I}}}^{0}u\,\mathrm{d}z=\frac{H_{\mathrm{i}}L}{\pi T}. \tag{13}$$

Since the motion is assumed to be rough-turbulent, the hydraulic gradient at the left-hand side of Eq. (12), δ/B, is proportional to the square of the transport velocity $V_{\mathrm{w}}=Q_W/h_{\mathrm{I}}$, and it is inversely proportional to D_{50}. According to Diskin et al. (1970), a bell-type function has been chosen to globally represent the effects of R_{c}, which influences both the amount of inflowing water and the magnitude of backflow resistances.

Yet, the maximum of the curve is now located at $R_{\mathrm{c}}=0$ instead of $R_{\mathrm{c}}=0.7H_0$ (Eq. (2)); the authors explained such a behavior as an effect of the breakwater permeability, which in their investigation was at least 40% larger than that of Diskin et al. (1970).

3. An alternative calculation method

3.1. Conclusions from literature analysis and description of the adopted approach

Apart from Eq. (2), which is purely empirical, in all the prediction methods presented earlier, the wave setup is interpreted as the force counteracting a structure-induced lack of momentum balance. The difference among them is on which force is considered to be the primary cause of the disequilibrium. Thus Longuet-Higgins focused on the flux of wave momentum, while in Loveless et al. (1998) formula, the mass flux is dominant and the shear stress related to the backflowing process is the main force. However, neither of the two approaches seem to be entirely convincing; the former, in fact, disregards wave breaking, as well as any dissipation source, while the weir-like scheme proposed by Loveless et al. (1998) appears more suitable for emerged breakwaters.

For these reasons, the Dalrymple and Dean (1971) procedure (D_2 hereafter) should be preferred in principle, as it accounts for both the breaking induced reduction of the wave momentum flux (radiation stress) and the mass balance. However, the following model shortcomings must be highlighted:

- Eq. (6) returns no momentum flux setup, δ_{mf}, for the very frequent case in which waves break at the top of the barrier ($h_{\mathrm{b}}=-R_{\mathrm{c}}$), and this sounds physically questionable.
- Since the momentum flux release continues while waves travel across the breakwater crown, δ_{mf} should also increase with B; in contrast, the crest width is not included in Eq. (6).
- The procedure does not consider either the transmission or the reflection coefficients, although the authors themselves underlined the relevance of these parameters.
- The high transport velocities, together with the roughness of materials which most of the breakwaters consist of, make the backflowing process hardly to occur without any dissipation. In this regard, it should also be mentioned that the thickness of the structures might reach considerable values, as in the case of the "artificial reefs" frequently adopted in Japanese practice.
- The procedure does not apply to random waves.

To cope with these problems, an alternative calculation method is presented and discussed in the following. The general structure of D_2 (Eq. (5)) is maintained, but the way of computing both the momentum flux and the continuity setup contributions is changed. In particular, δ_{mf} is calculated by applying the horizontal momentum balance to a control volume surrounding the structure, that allows including K_{R}, K_{t} and, indirectly, B in the computation. As far as the continuity contribution is concerned, it is modelled as the hydraulic head that is necessary to equilibrate the flow resistances due to the interaction between the undertow compensating the mass influx, and the structure. Finally, by use of irregular wave experiments, the "new" method is adapted to random seas.

3.2. The momentum flux contribution

To calculate δ_{mf}, the time-averaged horizontal momentum balance, per unit of span, has been applied to the control volume shown in Fig. 2, which is included between the sea bottom, the free surface, and the outer profile of the structure. The balance equation reads

$$S_{xx,\mathrm{II}}-S_{xx,\mathrm{I}}-\Delta\Pi+P_{\mathrm{II}}-P_{\mathrm{I}}=0, \tag{14}$$

where $S_{xx,\mathrm{I-II}}$ are the xx components of the radiation stress tensor (Longuet-Higgins and Stewart, 1962) at the vertical planes I and II, $\Delta\Pi$ is the net (horizontal) force exerted by the structure on the volume of fluid and $P_{\mathrm{I-II}}$ represent the external hydrostatic thrusts.

In calculating previous terms, some rough hypotheses are introduced. First, we assume the wave period to be an invariant of the process, that is, generation of high frequency free waves in the sheltered area (Grue, 1992) is not considered. It might be of interest that the writers have recently observed this assumption to be reasonable when heavy plunging breakers occur at the crest or at the seaward slope of a barrier (Calabrese et al., 2006). Furthermore, a partial standing wave field (*PSf* hereafter) is thought to take place in Region 1 of Fig. 2, while simple progressive waves are supposed for Region 2. For the radiation stress components, the following approximate expression is used at plane I:

$$S_{xx,\mathrm{I}}=S_{xx,\mathrm{i}}(1+K_{\mathrm{R}}^2)=\frac{1}{16}\rho_{\mathrm{w}}gH_{\mathrm{i}}^2\left[1+\frac{4k_{\mathrm{I}}h_{\mathrm{I}}}{\mathrm{senh}(2k_{\mathrm{I}}h_{\mathrm{I}})}\right](1+K_{\mathrm{R}}^2), \tag{15}$$

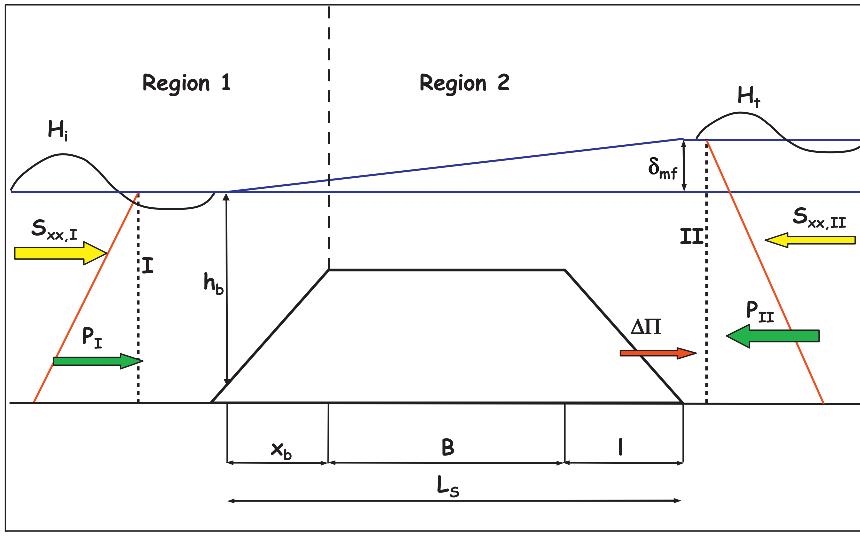

Fig. 2. Scheme for calculation of the momentum flux setup.

which is based on averaging the wave momentum flux over a wavelength, neglecting the shift of the phase constant between incident and reflected waves; note that for the limit cases of simple progressive waves ($K_R = 0$) and standing waves ($K_R = 1$), Eq. (15) returns the theoretical expressions found by Longuet-Higgins and Stewart (1964). Clearly, at plane II we have

$$S_{xx,\mathrm{II}} = S_{xx,\mathrm{i}} K_T^2 = \frac{1}{16}\rho_w g H_i^2 \left[1 + \frac{4k_{\mathrm{II}}h_{\mathrm{II}}}{\mathrm{senh}(2k_{\mathrm{II}}h_{\mathrm{II}})}\right] K_T^2. \qquad (16)$$

In estimating $\Delta\Pi$, we consider, as a first gross approximation, only terms related to the mean hydrostatic pressures; that means assuming all the other forces (mean dynamic pressures as well as average Reynolds stresses related to the through-passing) to vanish in their integral values along the breakwater, or to be negligible.

For the computation, we additionally suppose that the surf zone extends from the breaking point to the inshore toe of the barrier and that wave setup linearly increases across it (Fig. 2). For estimating the still water depth at incipient breaking h_b, the following procedure is adopted. It is assumed that waves collapse onto the front slope of the breakwater where the incident wave height equals the limiting value proposed by Iwata and Kiyono (1985):

$$H_i = \frac{1}{1+K_R}\left[0.218 - 0.076\,\frac{1-K_R}{1+K_R}\right] L_b \tanh\left(2\pi \frac{h_b}{L_b}\right), \qquad (17)$$

where L_b is the wavelength at incipient breaking, calculated through the linear dispersion relationship.

Iwata and Kiyono (1985) criterion has been chosen, because it explicitly includes effects of reflection, which dominates the wave motion seaward the breakwater crown. The formula returns the well-known Miche breaking criterion for progressive waves ($K_R = 0$) and the Daniel's (1952) formula for standing waves ($K_R = 1$). It is noteworthy that in deriving Eq. (17) wave shoaling on the front slope has been neglected; this is because it has been reasonably assumed the breakwater face to be so short and steep that waves have no time to change their height according to the abrupt variation of water depth (see Appendix A for further discussion). Additionally the front face of the breakwater has been thought to be a quasi-antinode of the *PSf* taking place in the Region 1 of Fig. 2.

If from Eq. (17), a value of h_b less than $|R_c|$ is obtained, then waves will not collapse onto the front slope; indeed the breaking might occur at the breakwater crest if H_i exceeds the Hur et al. (2003) limit wave height:

$$H_b^{\mathrm{cr.}} = 0.095 L_0 \tanh\left(\frac{2\pi|R_c|}{L_0}\right), \qquad (18)$$

where L_0 is the deep water wavelength. Eq. (18) comes from specific experiments on wave breaking at the crown of a submerged obstacle, though the model used in the Hur et al. (2003) research was smooth and impermeable. We see that under the feasible hypothesis of shallow water, Eq. (18) returns wave height to depth ratios of about 0.6. This corroborates findings of Sawaragi (1995), who analyzed the behavior of small and medium scale models of Niigata and Nishiki submerged breakwaters and found that wave breaking took place for $H_i/|R_c|$ around 0.625. Note that if we had simply used the Iwata and Kiyono formula for progressive waves ($K_R = 0$) we would have found $H_i/|R_c| \cong 0.87$, that is quite larger. This explains why we employed two different formulae for modelling wave breaking occurrence.

Finally, if incident wave height is less than the right-hand side of Eq. (18), the waves will travel across the structure without breaking and δ_{mf} as well as the total setup is set equal to zero.

As far as hydrostatic thrusts at planes I and II are concerned, they can be readily calculated from the triangular pressure distributions displayed in Fig. 2; in this regard, we make the further assumption of neglecting the wave setup in I, though in the offshore zone the mean water level actually fluctuates, owing to wave reflection.

Altogether, under the hypotheses enumerated earlier, Eq. (14) results in a simple second order equation in δ_{mf}. It has a unique positive solution, which for the simplest case of flat bottom ($h_I \equiv h_I \equiv h$) reads:

$$\delta_{mf} = 0.5\left[-b + \sqrt{(b^2 - 4c)}\right], \qquad (19)$$

where (Fig. 2)

$$b = (2h - A), \qquad (20)$$

$$A = \left\{\left[1 + \frac{x_b + B}{L_s}\right] h_c - \left[x_b\,\frac{h_b + R_c}{L_s}\right]\right\}, \qquad (21)$$

$$c = -\frac{1}{8} H_i^2 \left[1 + \frac{4kh}{\mathrm{senh}(2kh)}\right](1 + K_R^2 - K_T^2). \qquad (22)$$

In Eq. (21), x_b is the distance between the breaking point and the seaward edge of the structure crown, which is known from Eqs. (17) and (18). Note that x_b is always positive.

For the sake of simplicity, we take $x_b = 0$ as the waves break on the crown (Eq. (18)), although several studies (e.g. Hattori and Sakai, 1994) indicate wave collapse to initiate somewhat forward.

3.3. The continuity setup

As widely reasoned in the literature, a leading point of 2D wave setup behind submerged breakwaters is the process of mass transport related to the wave–structure interaction. When waves travel across the barrier and eventually break, an amount of water is pumped forward, that must be conveyed back, by a return current, to ensure the mass continuity.

Unlike D_2, we assume the interaction between return current and barrier, even if it is impermeable, to cause a shear stress that must be compensated by an increase of the hydrostatic thrust in the sheltered area. In this approach, a hydraulic resistance law is chosen for calculating the "continuity setup," δ_c, that is

$$\delta_c = \frac{q_{in}^2}{f^2 |R_c|^{10/3}} B_{eq}. \qquad (23)$$

Eq. (23) is known as the "Gauckler–Strickler formula" for uniform turbulent flows; in this expression, q_{in} is the volume influx to be balanced and f represents a friction parameter, inverse of the Manning's roughness factor, which has the dimensions of a $(\text{length})^{1/3}$ divided by a time.

The formula assumes the backflow to dominantly occur between the crest of the breakwater and the still water level; accordingly $|R_c|$ is used as hydraulic radius. Furthermore, the actual trapezoidal shape of the cross-section is replaced by an equivalent rectangular one, the width of which, B_{eq}, equals the ratio between the area of the cross-section, A_c and the breakwater height, h_c.

As far as the computation of q_{in} is concerned, we already mentioned that Dalrymple and Dean (1971), and Loveless et al. (1998) as well, somehow assumed the barrier to behave like a weir, that seems more appropriate for emerged breakwaters.

On the other hand, the authors noted, by inspection of a good deal of video recordings (see Pasanisi et al., 2006 for details), that breaker profiles on a submerged breakwater do not differ substantially from those observed on sloping beaches; for well submerged barriers and steep waves, spilling–plunging breakers take place on the crest (Fig. 3(a)), while, for longer periods, bore-like waves with an evident surface roller seem to occur (Fig. 3(b)). Finally, as soon as submergence reduces, plunging or collapsing breakers may take place on the front face, depending on both slope angle and permeability (Figs. 3(c) and (d)).

With this in mind, and owing to a substantial lack of knowledge for the specific case of submerged breakwaters, the general theory of mass transport in the surf zone has been referred to for calculating the net influx.

In general, according to Svendsen (1984), the total mass drift of a breaker of height H, including both the orbital motion and the surface roller contributions, can be expressed as

$$q_{in} = \sqrt{\frac{g}{h^*}} H^2 \left(B_0 + \frac{A_r}{H^2} \frac{h^*}{L^*} \right), \qquad (24)$$

where h^* is a generic water depth, L^* represents the wavelength at depth h^* and A_r is the area of the surface roller in the vertical plane; B_0 is a shape factor that for sine waves equals 0.125 and diminishes as soon as the peakedness of the waves increases (Buhr-Hansen, 1990). Regarding the surface roller contribution, Okayasu (1989) proposed setting $A_r = 0.06 \cdot H \cdot L^*$, that leads to

$$q_{in} = \sqrt{g h^*} H \left(B_0 \frac{H}{h^*} + 0.06 \right). \qquad (25)$$

When introducing Eq. (25) into Eq. (23), the water depth, h^*, is approximated with the submergence $|R_c|$ and the average wave

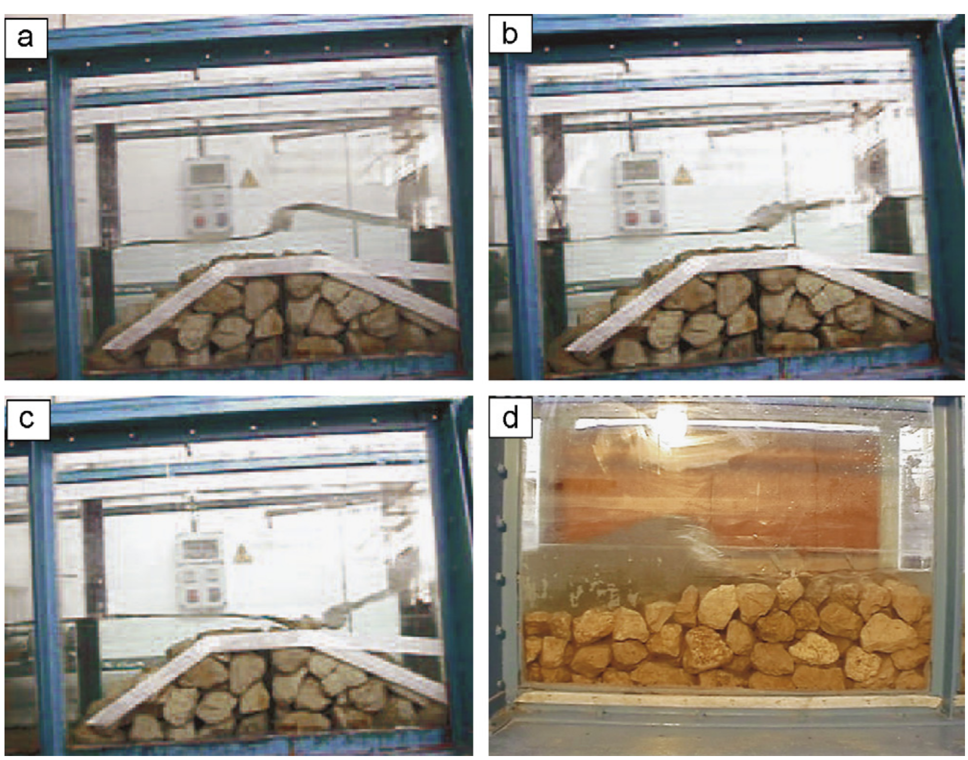

Fig. 3. Breaker types at a submerged breakwater: (a) spilling–plunging, (b) bore, (c) collapsing, and (d) plunging on the front slope.

height along the structure, $\overline{H}=H_i(1+K_t)/2$, is used for H. The latter because as the wave decays across the barrier, the mass transport reduces as well and the mean return current (undertow) that locally balances the mass influx, induces a unitary shear stress on the structure, which also decreases along the breakwater. Therefore, since Eq. (23) basically deals with the integral (resultant) value of the shear stress, the mean wave height is used in the computation at a first approximation level.

B_0 and f are left as unspecified parameters to be calibrated from experimental data; accordingly their values will smooth the effects of the crude hypotheses we introduced earlier. However, because they play a key role in the proposed model, a general discussion about their order of magnitude could be of course useful. This issue is addressed in the following section.

3.4. Expected values of B_0 and f

It has been already stated that B_0 is a wave shape factor, which parameterizes the peakedness of waves. Although no theory exists for predicting its value in the surf zone, we may obtain some useful indication through the cnoidal wave theory, which gives B_0 as a function of the Ursell parameter U_R. Here the following approximate expression can be employed:

$$B_0 = 0.125\tanh\left(\frac{11.40}{\sqrt{U_R}}\right), \tag{26}$$

which is accurate within $\pm 2\%$ for $U_R < 2000$. Buhr-Hansen (1990) found the equation above to furnish a reliable estimate of B_0 at the breaking point; hence we might reason it could be used as a reference for narrow crested breakwaters, where wave transformation after breaking is expected to be small.

If we assume the breaking point to be located not far from the crest, then Ursell factor can be written as:

$$\begin{aligned} U_R &\equiv \frac{HL^2}{h^3} \cong \frac{H_i[gT^2(H_i+|R_c|)]}{|R_c|^3} \\ &= \frac{2\pi}{s_0}\left(\frac{H_i}{|R_c|}\right)^2\left(1+\frac{H_i}{|R_c|}\right), \end{aligned} \tag{27}$$

where it has been set $L=[g(H_i+|R_c|)]^{0.5}T$ and $s_0 = H_i/L_0$. If the latter varies in the realistic interval 0.01–0.04, B_0 should not be larger than 0.039–0.071, for $H_i/|R_c|$ is hardly less than 1 in practice. It is also clear that as soon as the structure thickness becomes large, previous values may be no longer valid; this because wave height evidently undergoes a deep transformation over the crown, the effects of which on B_0 are very difficult to foresee.

As far as the friction factor f is concerned, predictions are even more complicate, mainly because of the lack of knowledge about the magnitude of the shear stress exerted by a submerged breakwater on the neighbouring fluid. However, with the aim of deriving a first rough estimate, a number of calculations have been tentatively performed, using different approaches. Results are summarized in Table 1. Rows 1–3 refer to empirical formulae calibrated on natural channels with coarse bed material and no significant vegetation (Lang et al., 2004). In these formulae, which are not consistent from a dimensional point of view, R is the hydraulic radius and D_x represents the diameter of bed material, for which x% of the diameters are equal or smaller. The fourth column of the table reports the maximum D_{50} used for the calibration of the formulas.

Rows 4–5 refer to a more specific coastal engineering context. In those research, the unitary shear stress at the bottom, τ_b, has been modelled by the expression $\frac{1}{2}\rho\lambda U_b^2$, where λ is a non-dimensional friction coefficient and U_b is the bottom velocity. Reference values for λ have been also provided by the authors. Now, it is noteworthy that in this study we have implicitly assumed $\tau_b = \rho g R S_w$, where S_w is the slope of the energy grade line; consequently, by using the Gauckler–Strickler formula for calculating S_w and by equating the two expressions of τ_b, we readily come to the relationship between λ and f reported in Table 1. Clearly, it holds only in the frame of a fully turbulent flow.

In calculating the expected values of f, it has been obviously assumed $R \equiv |R_c|$; moreover, since we are looking for the order of magnitude of friction factor, it has been realistically set $|R_c|^{1/6} \approx 1$ and $|R_c|/D_x \approx 1$, for whatever x.

Altogether the inspection of Table 1 reveals that order of magnitude of f should be likely $10\,\mathrm{m}^{1/3}/\mathrm{s}$. Note that this value refers to prototype conditions; it must be properly scaled in laboratory experiments. In this regard we note the since the actual dissipative processes associated with the shear stress are of a purely turbulent nature, they should be in similitude in an ideal Froude-scaled geometrically undistorted model. Consequently, the scale ratio of f should be $N_L^{-1/6}$(N_L is the prototype to model length scale ratio), though we cannot exclude, in principle, the presence of transitional boundary layers in the small-scale experiments.

However, to avoid any confusion and facilitate the application of the model, in the following all the experimental results are discussed with reference to the prototype conditions; a discussion on possible scale effects is given at the end of the paper.

Before concluding this section, it should be also highlighted that in our approach f accounts the energy loss due to the interaction between the return current and the structure, in a

Table 1
Expected values of the friction factor f

Author(s)	Formula.	Valid for	Max D_{50} (m)	Expected for ($\mathrm{m}^{1/3}$/s)
Limerinos	$f=\frac{1.16+2.0\log(R/D_{84})}{0.113R^{1/6}}$	Natural channels	0.253	10
Griffiths	$f=\frac{0.760+1.98\log(R/D_{50})}{0.113R^{1/6}}$	Natural channels	0.301	7
Phillips and Ingersoll	$f=\frac{1.46+2.23\log(R/D_{50})}{0.113R^{1/6}}$	Natural channels	1.181	13
Nelson (1996)	$f=\sqrt{\frac{2g}{\lambda R^{1/3}}};\quad \lambda=0.1-0.2$	Coral reefs	–	10–14
Lamberti et al. (2007)	$f=\sqrt{\frac{2g}{\lambda R^{1/3}}};\quad \lambda=0.25-0.35$	LCBs	Qualitative suggestion	7–9

"global manner". Then also permeability is expected to affect its value, although it has been formally ignored when the model has been derived. In general, the larger the permeability, the lower the setup is expected to be; this because of the increase of the flow section available for backflow, that reduces transport velocity and, accordingly, the shear stress. This effect should also prevail on the expected increase of wave influx due to more transmission that, oppositely, would increase the wave setup.

In short, the variation of structure permeability leads to a variation of the shear stress induced by the structure on the surrounding fluid; in the model, this effect is accounted through a variation of friction parameter f, which would increase (less friction) with increasing permeability. More details on this matter are given in the subsequent sections.

4. Experiments

With the aim of calibrating and validating the new model, as well as for investigating its applicability to random seas, four data sets, coming from experiments conducted at three different laboratories, have been gathered. The whole database sums 362 hydraulic model tests.

The Bristol small-scale experiments (scale 1:20) have been carried out at the Hydraulics Laboratory of University of Bristol's Civil Engineering Department. The experimental study has been completed for the UK Ministry of Agriculture, Fisheries and Food, and it is described in details in Loveless and Debski (1997). The flume used to perform the tests is 15 m long, 1.5 m wide and 1.1 m high. Altogether, eight different models were tested, including variations in crest width, still water level, slope angles and rock size. All the cross-sections were homogeneous. Most of the experiments were conducted with regular waves, but some irregular wave tests were also run. Results from regular wave experiments were used for calibrating the Loveless et al. (1998) formula (Eq. (12)). Although both positive and negative clearances were tested, only the experiments conducted on submerged breakwaters have been used here.

Large-scale GWK experiments (approximate scale 1:2) were conducted by the writers at the Grosser WellenKanal of Hannover (Germany), in the frame of the EU project *Submerged and Low-Crested Breakwaters in Presence of Broken Waves* (Calabrese et al., 2002). GWK flume is 307 m long, 5 m wide and 7 m deep, and water waves up to a height of 2 m can be simulated under a "quasi-prototype" condition. The facility is also equipped with a "double loop" online active absorption system. The structure cross-section consisted of a core and an armour layer; two crest widths were considered, namely 1 and 4 m (2 and 8 m at a prototype scale) and both the front and rear slopes were 1:2. The models were subjected to random waves ranging from prebreaking to broken. Although both submerged and subaerial configurations have been tested, only underwater structures have been considered for the scopes of the present work.

Supplementary small-scale regular wave tests (scale 1:20) were conducted at the University of Naples "Federico II" (Pasanisi et al., 2006; Di Pace, 2006); they will be referred to as UoN tests hereafter. Twenty of them have been already presented in Calabrese et al. (2005), whereas 64 are discussed here for the first time. The flume where experiments have been carried out is 23.50 m long, 0.5 m wide and 0.75 m high; the wave generation system, capable of generating both regular and irregular waves, is provided with an active wave absorption system. Two models of homogeneous rubble mound submerged breakwaters have been tested with waves of different heights and periods. The models differed by crown width (0.25 and 0.35 m, respectively) and by crest freeboard (0.065 and 0.055 m, respectively). The front slope was 1:2 and the rear one was 1:1.5 for both the structures. To investigate the effects of the permeability, tests with the shorter model have been repeated after having inserted a wooden impermeable plate in the body of the barrier. Two different heights of the plate have been employed, namely h_c and $h_c/2$.

In all the experiments, passive wave absorbers were located at the end of the flumes and wave profiles were acquired in front and at the rear of the structures. The wave setup in the sheltered area, δ, has been obtained by time averaging wave profiles in the interval where the mean water level was seen to be constant. Actually, before this stationary condition is reached, the mean sea level progressively ramps up due to a temporary misbalance between influx and backflow.

For Bristol's regular wave tests, incident and reflected wave heights were separated by using a single probe mounted on a trolley and moved offshore the breakwater along nine positions over half the incident wavelength. For Bristol's random experiments and UoN, the Mansard and Funke (1980) technique was applied; as far as GWK tests are concerned, the presence of wave breaking on the foreshore was thought to significantly affect the reflection analysis, and consequently K_R were not evaluated. Here the incident wave height was estimated (spectrally) by repeating the tests in the absence of structure, and by retaining only the part of the power spectrum at frequencies larger than half the offshore peak one. Transmitted waves were measured at a single location for Bristol and UoN and at three different points for GWK; for these tests, both the wave setup and the transmitted wave height (calculated from the high frequency spectrum) were defined by averaging results coming from the three probes.

Table 2 provides a summary of the main characteristics of the data sets. The suffix "i" stands for "incident", while L_p and H_{rms}, respectively, represent the peak wavelength and the "energetically equivalent" wave height $H_{rms} = \sqrt{8m_0}$, where m_0 is the zero order spectral moment. For UoN, H_{rms} has been used for approximating the crest to trough wave height, H, either incident, or reflected, or transmitted. For Bristol regular wave experiments, a zero crossing method has been apparently used for estimating both the incident and the reflected wave heights, whereas H_{rms} has been used for the transmitted one.

5. Performances of the new method under regular waves

5.1. Permeable (conventional) breakwaters

The new model has been initially best-fitted to Bristol regular wave experiments and the values of 0.02 and 6 $m^{1/3}/s$ have been estimated for B_0 and f, respectively. On the whole the value of

Table 2
Database characteristics (prototype values)

Data set (wave type)	$D_{50,a}$ (m)	$D_{50,c}$ (m)	Front slope	Rear slope	$h_i/L_{(p)i}$	$-R_c/H_{(rms)i}$	$B/H_{(rms)i}$	Nr.
Bristol (reg.)	0.7–1.0	–	0.33–0.5	0.5–0.67	0.10–0.42	0.3–3.3	1.1–13.2	216
Bristol (ran.)	0.7–1.0	–	0.33–0.5	0.5–0.67	0.08–0.23	0.5–3.4	3.6–10.6	37
GWK (ran.)	0.44	0.14	0.5	0.5	0.06–0.13	0.3–1.1	1.5–10.9	25
UoN (reg.)	1.2	–	0.5	0.67	0.09–0.23	0.4–1.1	2.0–5.3	84

roughness parameter is consistent with our previous estimates, while B_0 is somewhat lower than what we expected. However, such a value of wave shape factor is not unrealistic, seeing that in analyzing variation of B_0 across sloping beaches, Basco and Yamashita (1986) found a value of B_0 very close to 0.02 for plunging breakers (at the breaking point).

Predicted and measured values of δ are compared in Fig. 4, which reveals a reasonable agreement, although some residual scatter exists; the latter might be partly due to the aforementioned non-homogeneity in the wave height definition.

However, when compared with Loveless et al. (1998) formula, which has been also calibrated on these data, the new method seems only slightly more reliable, giving a standard error, SE (standard deviation of difference between measured and predicted values), of 0.080 m vs. 0.087 m and an $R^2 = 0.84$ vs. 0.82. Nevertheless, when UoN data are dealt with (homogeneous breakwaters only without wooden plate; 42 data), it can still provide good predictions, with the same values of parameters, while Loveless et al. (1998) formula returns significant underestimates (Fig. 5).

In Table 3, the performances of all the prediction methods reviewed in Section 1, as well as of our approach, are compared. Together with SE and R^2, also the bias, mean of differences between measured and predicted values of wave setup, is considered. This is to measure the tendency of formulae at underpredicting (positive bias) or overpredicting (negative bias) the experimental data. Whether UoN or all data are considered, the new formula seems the best performing, as it is practically unbiased, with the minimum SE and the maximum R^2. As previously observed, the equation of Loveless et al. (1998) is probably too empirical, while D$_2$ seems to have a reasonable predictive power that confirms the effectiveness of the authors' approach.

As far as Diskin et al. (1970) formula is concerned, we note it to be more reliable when the incident wave height, H_i, is used (see "Diskin et al. (1970) with H_i", in Table 3) instead of the deep water one, H_0. It is also worth noting that the quality of predictions seems to be little influenced by wave reflection. This is clear when reliability indexes of Table 2 last row are compared with those of the "complete" model (first row). The reason why this happens is because K_R acts on two terms of the momentum equation, which tend to balance. From a side the larger the reflection coefficient, the larger the shoreward oriented force at the vertical plane I due to radiation stress (Eq. (15)); otherwise, with increasing reflection, the breaking point moves seaward (Eq. (17)), causing an additional thrust, offshore directed, exerted by the structure on the volume of fluid. Consequently, by also considering the lack of reliable equations for calculating K_R at submerged breakwaters

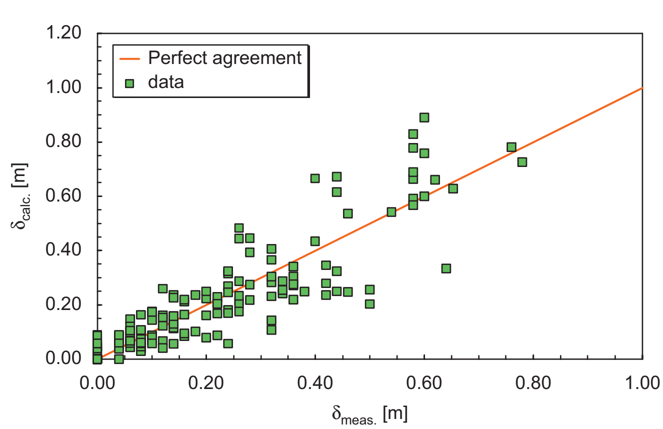

Fig. 4. The new model compared with Bristol's regular wave data.

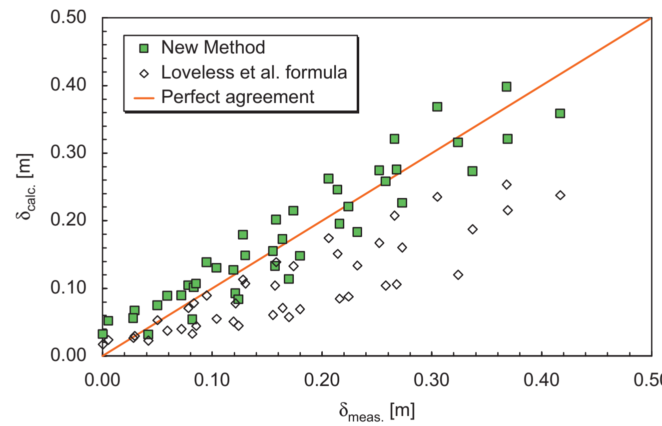

Fig. 5. The new model and Loveless et al. (1998) formula compared with UoN data.

Table 3
Reliability of prediction methods (database size: 320 data)

Prediction method	Data	BIAS (m)	SE (m)	R^2
New method	UoN	−0.006	0.035	0.89
	All data	−0.004	0.076	0.84
Diskin et al. (1970)	UoN	−0.045	0.073	0.65
	All data	−0.042	0.105	0.75
D_2	UoN	−0.020	0.050	0.78
	All data	−0.007	0.089	0.74
Loveless et al. (1998)	UoN	0.068	0.058	0.78
	All data	−0.009	0.089	0.79
Diskin et al. (1970) with H_i	UoN	−0.024	0.049	0.81
	All data	−0.021	0.088	0.79
New method with no reflection	UoN	−0.002	0.038	0.87
	All data	−0.001	0.076	0.81

(recently some indications have been provided by Zanuttigh and van der Meer, 2006), wave reflection might be neglected in practical applications.

Before proceeding with discussion it is necessary to remark that present work has not commented on the model proposed by Bellotti (2004), which uses the structure induced wave setup as a variable to address the problem of the rip currents through the gaps of a segmented system of submerged breakwaters. This is because, as a consequence of having employed the shallow water equations, Bellotti's method includes a friction term (shear stress), which vanishes as soon as the structure length increases. This makes the model inherently inadequate for 2D flow conditions (i.e. when the structure length is theoretically infinite), where it has been seen to give heavy underpredictions. However, the authors are aware that Bellotti is currently improving his method, just to cope with this problem. Once the new model is published it will be extremely interesting to compare its predictions against our method.

5.2. *Effects of permeability on friction parameter f*

As mentioned earlier in our approach the friction parameter is expected to become lower (that means more friction) as soon as the structure permeability reduces. This basically accounts the increasing of the shear stress exerted by the structure on the water because of the reduction of the flow section available for backflow. In other words, when permeability of the structure decreases, instead of reducing the hydraulic radius in Eq. (23), we decrease the friction coefficient f, leaving the hydraulic radius (which has been set equal to $|R_c|$) unchanged. The relation between the roughness factor and the hydraulic conductivity of the barrier has been partially studied by using the two series of UoN experiments where two wooden plates were installed into the cross-section of the breakwater. The heights of the plates, h_P, were equal to the breakwater height, $h_P/h_c = 1$, and to half of the breakwater height, $h_P/h_c = 0.5$, respectively. When the formulae have been best-fitted to the data, the values $f = 5.0$ and $3.8\ \mathrm{m}^{1/3}/\mathrm{s}$ have been found for the semipermeable and impermeable structure, respectively. This confirms that the reduction of hydraulic conductivity leads to an increase of wave setup. Predictions of the "re-calibrated model" are compared with measured values in Fig. 6(a), while the friction parameter is reported in Fig. 6(b), as a function of h_P/h_c.

Despite the very good agreement shown in Fig. 6(a), which, however, underlines the model capability of fitting the experimental data, previous results must be considered but general indications that are of a purely qualitative nature. This is mainly because the permeability has been here modulated without changing the porosity; oppositely in most of the practical cases, the reduction of hydraulic conductivity is accompanied by a reduction of voids volume. Thus, more experiments are recommended to develop relationships with an acceptable level of robustness.

6. Adaptation of the new model to random seas

Since this study deals with an engineering approach to computing wave setup, the adaptation of predictive equations to random waves will be pursued to seek a single wave descriptor (wave height and period), which is representative of the entire sea-state both seaward and leeward of the breakwater. In this regard, Thompson and Vincent (1985) argued that there is no intrinsic relationship between regular and irregular wave parameters, and accordingly their equivalence depends on which wave feature may be considered as the primary concern. In the opinion of the authors, the choice of the representative wave quantities for the present matter can only be established on an empirical basis. This is because the wave setup development in the protected area has been seen to depend on both wave energy dissipation and mass transport processes; consequently, if, for instance, $H_{\mathrm{rms}} = \sqrt{8m_0}$ is chosen, an equivalence between regular and irregular wave energy is ensured, but the equivalence of mass transport is evidently not guaranteed. Hence, a modification of model parameters might be required to counteract this effect. On the other hand, it is of interest that Loveless and Debski (1997), comparing results of the Bristol regular and random wave experiments, concluded that "the results of regular wave tests may be used with reasonable accuracy to predict the setup due to random wave series of average wave height equal to the regular wave height".

As a consequence of the above statements, two "equivalent wave heights" have been considered, namely H_{rms} and the average wave height, H_{μ}; note that under the hypothesis of Rayleigh distribution $H_{\mu} = \sqrt{\pi/4}\,H_{\mathrm{rms}}$. Clearly, the equivalence applies to both the incident and the transmitted wave heights.

Regardless of the selected wave height statistics, the peak period, T_p, has been used, since, according to our hypothesis, it remains nearly constant across the structure. The transmission coefficient, defined as the square root of the transmitted to incident wave energy ratio has also been treated as an invariant of the problem, and finally, wave reflection effects have been neglected for the sake of simplicity.

However, even after the above assumptions have been introduced, the problem still remains to define the "breaking point" of the representative wave. In this sense, it is widely known that for a random wave parameter (e.g. the significant wave height), the locution "incipient breaking condition" holds but in the sense that when a given amount of waves in the sea-state have physically broken, the wave descriptor starts to decay in a way quite similar to a regular wave. This is shown in Thompson and Vincent (1985) and, above all, in Kamphuis (1991). Now the sense of looking for a random breaking criterion to introduce in the momentum balance Eq. (15) is that we suppose the wave setup (and all the forces related to it) to be statistically negligible before the equivalent wave height has commenced to reduce.

As far as the quantitative indications are concerned, Kamphuis (1991) noted the "breaking point" of H_{rms} to be the same as for the significant wave height and proposed the following limiting criterion for straight slopes:

$$\left(\frac{H_{\mathrm{rms}}}{h}\right)_{\mathrm{b}} = \frac{1}{\sqrt{2}}\left(\frac{H_s}{h}\right)_{\mathrm{b}} = 0.40\exp(3.5m), \tag{28}$$

where m represents the bottom slope. Because of the lack of knowledge for the specific case of a submerged breakwater,

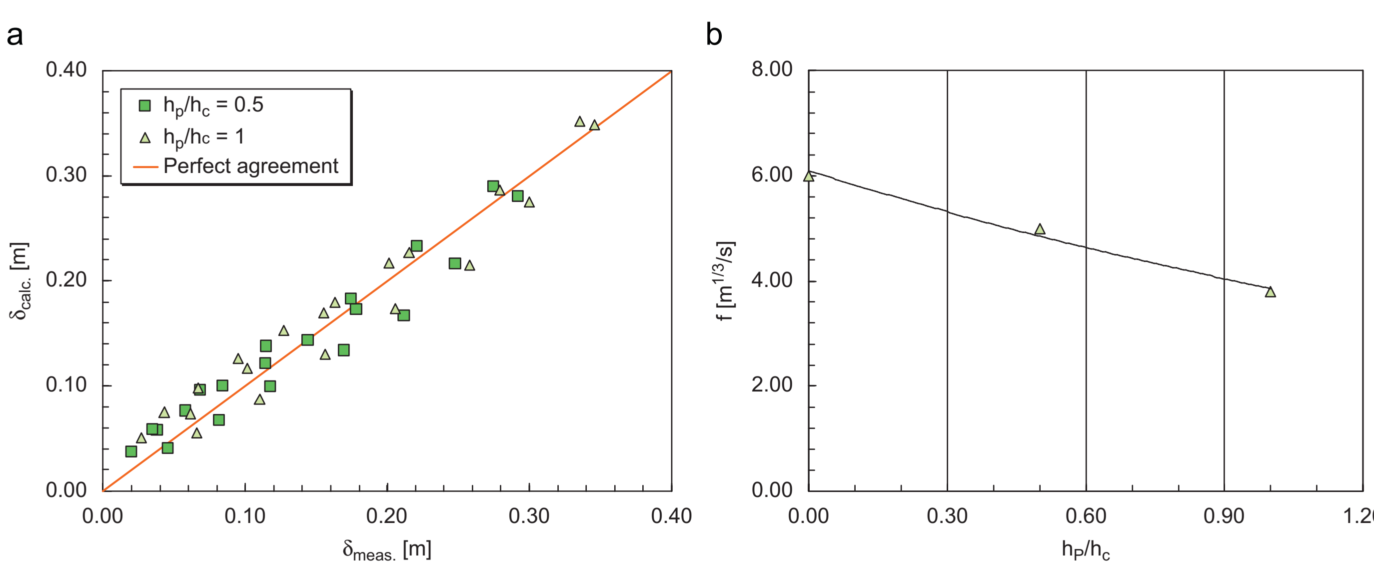

Fig. 6. Effect of permeability on friction parameter, f: (a) comparison between the new method and data, and (b) f as a function of structure permeability.

Eq. (26) has been employed as a breaking criterion for H_{rms}; we set $m = \tan\alpha_{off}$ for the front slope and $m = 0$ when wave collapsing onto the breakwater crown is considered. Regarding H_{μ}, since it is only weakly smaller than H_{rms}, we may reasonably suppose its breaking point to be the same. This leads to

$$\left(\frac{H_{\mu}}{h}\right)_{b} = \sqrt{\frac{\pi}{4}}\left(\frac{H_{rms}}{h}\right)_{b} = 0.35\exp(3.5m). \quad (29)$$

Application of the new procedure has shown that when the energetically equivalent wave height is used, a slight recalibration of the friction parameter is needed, its best-fit value being equal to 8.5 $m^{1/3}$/s. This was partly expected. Otherwise, when the mean wave height is chosen, it returns good estimates of wave setup, without changing any coefficients. That basically confirms the findings of Loveless and Debski (1997). In both cases, a very satisfactory agreement is detected, SE being around 0.024 m and R^2 close to 0.95 (Figs. 7 and 8). This is somewhat surprising, given the supplementary and rather crude hypotheses we had to introduce.

7. Discussion and conclusions

This study has presented a new method for calculating the 2D wave setup behind a submerged breakwater. Starting from a conceptual scheme originally proposed by Dalrymple and Dean (1971) (D_2, Eq. (5)), the method decomposes the whole setup into two parts, namely the "momentum flux" contribution, δ_{mf}, and the "continuity setup", δ_c; the former is related to the reduction of wave momentum flux forced by wave breaking, whereas the latter is associated with mass transport process. The momentum flux contribution has been calculated by applying the balance of the horizontal momentum to a control volume surrounding the structure; two different breaking criteria have been used, depending on whether the wave collapse occurs at the front face or at the crown of the barrier, and both the transmission and the reflection coefficients have been explicitly included in the predictive equations (Eqs. (19)–(22)). For "continuity setup," δ_c (Eq. (23)), it has been interpreted as an additional specific hydrostatic thrust required to counteract the shear stress due to the interaction between the return current and the structure.

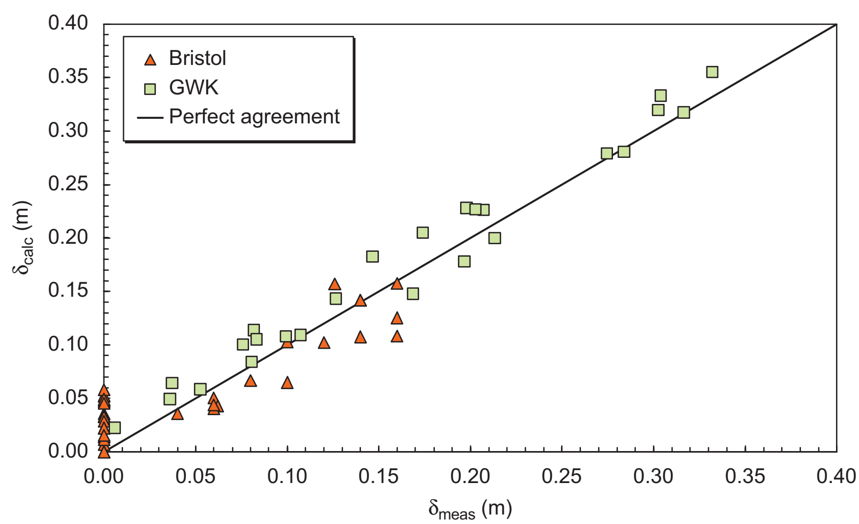

Fig. 7. Adaptation of the new method to random seas using H_{rms}. $f = 8.5\,m^{1/3}/s$.

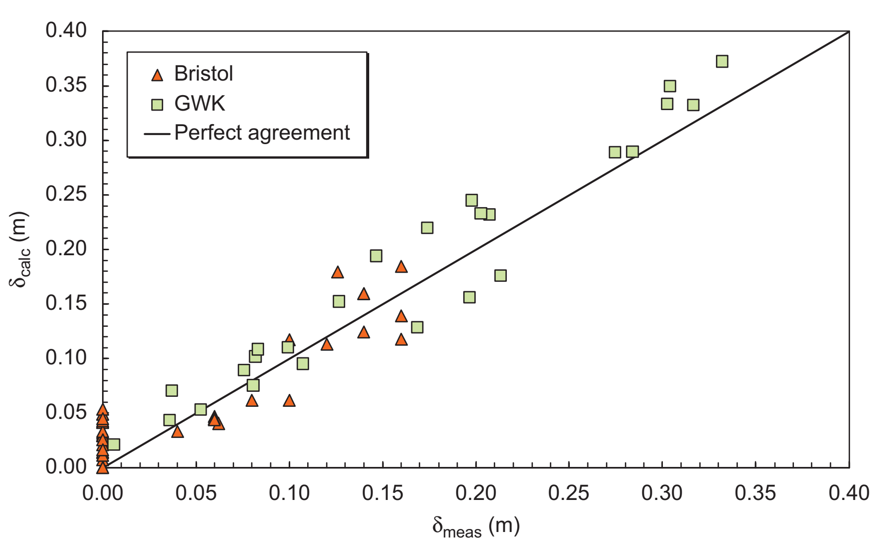

Fig. 8. Adaptation of the new method to random seas using H_{μ}. No recalibration of parameters.

Accordingly, the influence of breakwater permeability has been accounted through the "global" friction parameter f.

Although derived for regular waves, the method has been heuristically extended to random seas by simply using appropriate sea-state descriptors, namely H_{rms} (or H_{μ}) and T_p, and a random wave breaking criterion (Eqs. (28) and (29)). More than 350 experiments from three different laboratories have been used to calibrate and verify the model, which seemed to fit well the data, often with a very satisfactory approximation (Figs. 5, 6(a), 7 and 8). However, three additional points deserve to be discussed; two of them concern model features, while the third is related to how present results may be used in the future research developments.

First, we have to note that model application is inherently limited by the value of crest freeboard, R_c. As soon as the crest level approaches, and possibly overcomes the still water level, the structure tends to behave more or less like a weir and the basic undertow scheme we adopted for δ_c fails; note that for $R_c = 0$, Eqs. (19)–(22) return an infinite wave setup. Hence, we recommend extreme caution when applying the model out of the experimental ranges reported in Table 1, and particularly for H_i/R_c (or $H_{(rms)i}/R_c$ when random waves are considered) larger than about 3.5 in absolute value. It may be of interest to confirm the above statement looking at the four experimental data reported in Table 1 of the Diskin et al. (1970) research. The comparison with the new method is reported in Table 4, assuming a 1:20 model scale and using d'Angremond et al. (1996) to calculate K_t. Predictions of new method are shortly referred to as δ_{2D}. As expected, the model is seen to give proper estimates until the absolute value of H_i/R_c is slightly larger than 3; for $H_i/R_c = 4.27$, it gives a heavy overprediction.

Another point to be commented is about scale effects. All the experiments we used in this study come from 1:20 models of submerged breakwaters except GWK, being at a quasi-prototype scale. Yet the latter includes multilayered cross-sections, whereas in small-scale experiments homogeneous barriers were employed. It is then a little surprising that experimental data in Figs. 7 and 8 compare well with model predictions, though a unique value of friction parameter f was used (6 $m^{1/3}$/s). Actually, as the permeability of GWK structures is likely smaller than in Bristol, we expected, according to Fig. 6(b), a lower value of f for those experiments. There are at least three possible explanations for this behavior. The first is that reduction of structure porosity (from nearly 0.4 for homogeneous breakwaters to likely 0.3 for a barrier with a core) causes a variation of permeability much smaller than in the case of an impermeable sheet inserted into the breakwater cross-section. The second is that a transitional boundary layer took place in the Bristol tests, giving rise to some scale effects. A third possible explanation may be the roughness of the armor units to have been significantly different between the two experimental series. Unfortunately, no definitive conclusions can be drawn about this major matter, which needs be deeply analyzed in the future research works.

Finally, it is worth discussing possible applications of the model, both in the practical engineering and research domains. Although it returns in principle the rise of the mean water level behind a submerged breakwater that completely closes the bay where it is located, other physical interpretations may be possible.

Table 4
New method vs. Diskin et al. (1970) data

Test number	H_0 (m)	T (s)	$H_i^{(*)}$ (m)	$-R_c$	$-H_i/R_c$	$K_t^{(**)}$	$\delta_{measured}$ (m)	δ_{2D} (m)
1	2.82	5.50	2.59	2.00	1.29	0.66	0.14	0.16
2	3.22	6.71	3.12	1.00	3.12	0.53	0.58	0.63
3	2.12	7.24	2.14	0.5	4.27	0.51	0.48	1.04
4	2.54	5.46	2.60	0	∞	0.35	0.80	∞

We observe that under the hypotheses of normally incident waves and straight parallel depth contours, the middle section of a breakwater system, of whatever (but finite) length, may be considered as a symmetry axis of the problem; accordingly, the flow motion will be there nearly 2D and, if effects of diffraction can be considered negligible, wave setup should approach δ_{2D}. Since the rise of the mean water level at the breakwater heads (or at gaps) is quite low, or possibly slightly negative, we see δ_{2D} might represent an estimate of the potential alongshore variation of the mean water level by which a given amount of water is conveyed parallel to the breakwater and then offshore; such a conclusion is consistent with the aforementioned field observations by Dean et al. (1997).

Hence, the authors believe that δ_{2D} might be used as a variable of simplified design equations, which aid engineers in calculating important flow parameters such as the alongshore velocity behind the structure or the flow speed through the gaps. The equations to be developed, which require a proper experimental calibration and validation, could be both empirical formulae and simplified circulation models.

To get an example of possible application the reader could refer to the aforementioned Lamberti et al. (2007) paper, where a simple circulation model is proposed, based on the generalized Bernoulli theorem to calculate the rip current velocity through the gaps of a segmented breakwater system (Eq. (13.92) of the paper). In that model δ_{2D} could be used as a potential value of the pressure behind the structure, ruling a potential rip current flow speed.

A further and more detailed example is given in Fig. 9, where the case of a single submerged breakwater is considered. If we assume that $\delta_{2D}/h_{II} \ll 1$ and that the structure is short enough in the alongshore direction to render the energy loss by friction negligible, the maximum velocity of the longshore current flowing behind the structure, V, might be obtained from the momentum balance in the y direction, applied to the volume of fluid shown in the graph. By invoking the symmetry condition at the centreline, it can be expressed as

$$\rho_w V^2 h_{II} = \rho g h_{II} \delta_{2D} - S_{yy,D} + S_{yy,t} = 0, \tag{30}$$

where $S_{yy,D;t}$ represents the yy component of the radiation stresses associated to the diffracted and transmitted waves, respectively. They may be roughly calculated by multiplying the incident radiation stress by the square of the local diffraction and transmission coefficients, K_D and K_t. This also implies that, as mentioned before, effects of diffraction are negligible for $y = 0$. Under the further hypothesis of shallow water, we obtain the following equations where V is directly related to δ_{2D}:

$$\frac{V}{\sqrt{g h_{II}}} = \alpha \left[\frac{\delta_{2D}}{h_{II}} - \frac{1}{16} \left(\frac{H_i}{h_{II}} \right)^2 (K_D^2 - K_t^2) \right]^{0.5}, \tag{31}$$

where α is an empirical correction coefficient (to be experimentally calibrated) accounting for all the neglected physics. Note that in developing a circulation model for barred beaches, Dalrymple (1978) used the same boundary conditions, that is, 2D motion at the central part of the bar and no setup at the gaps.

Note Eq. (31) holds only if the right-hand side of Eq. (30) is positive; if not, the current will be directed towards the shadow zone and a salient possibly forms. Note that in accordance with the simplified scheme of Fig. 9, a net influx $Q_{IN} = V h_{II} l$ is required to close the mass balance, where l is the width of the zone where the water flow takes place; Diskin et al. (1970) suggested $l \approx 4$–$6h_c$. Moreover, it should be noted that if the flow at the middle section

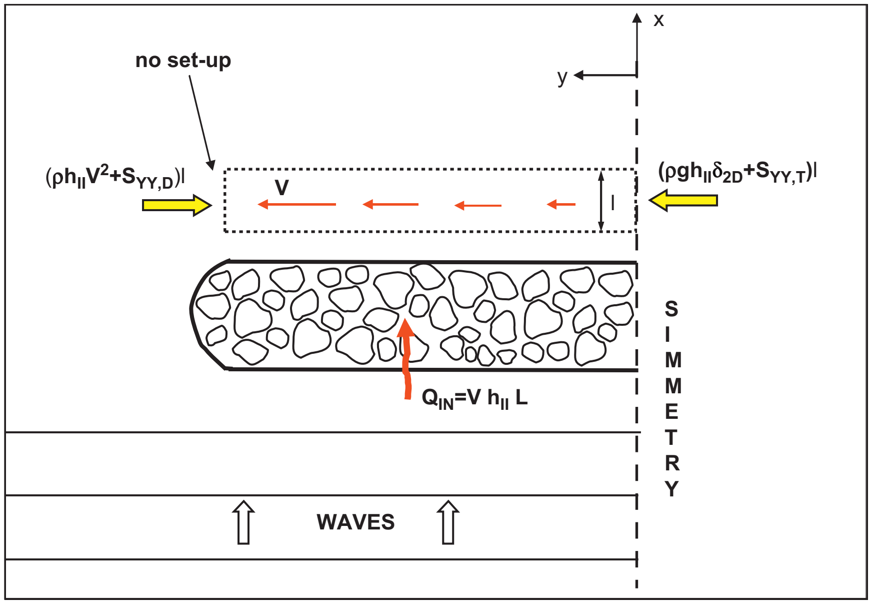

Fig. 9. Longshore current behind a single submerged breakwater.

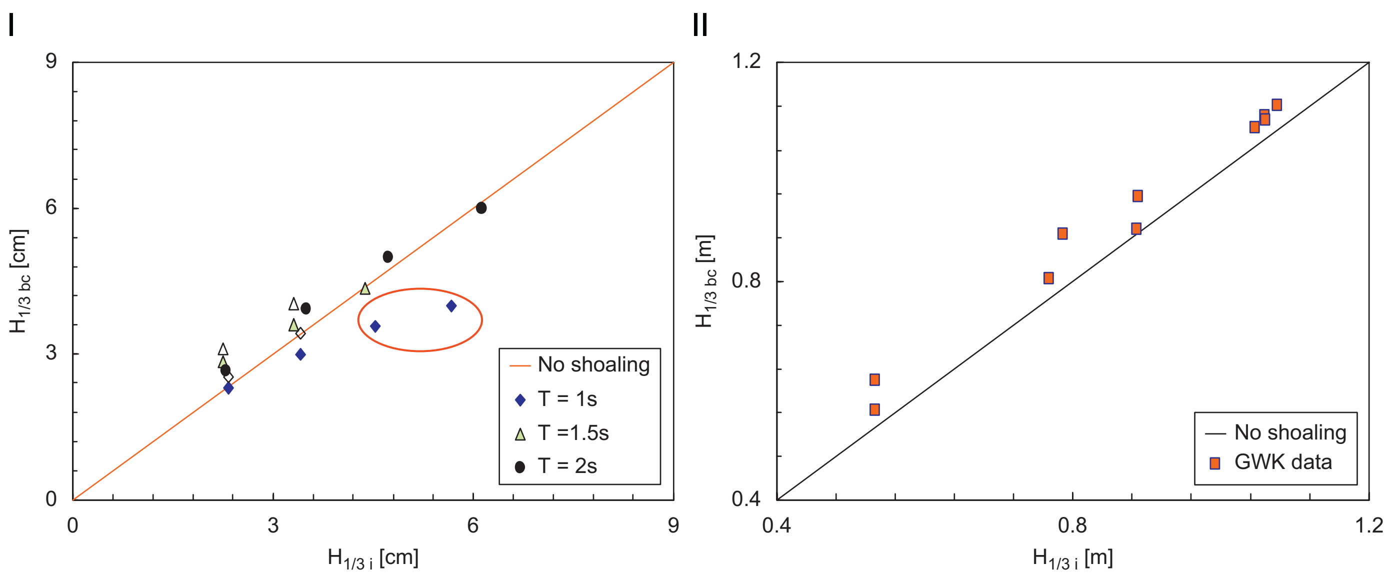

Fig. A1. Wave transformation on the front slope of submerged breakwaters (data at model scale). (I) UoN data: solid symbols refer to permeable breakwater, open symbols refer to $h_P/h_c = 1$. (II) GWK data

could not be considered 2D, then δ_{mf} instead of the entire δ_{2D} might be used.

Despite the above circulation model being extremely crude, it clearly shows that the findings of the present study can be used in developing more powerful design tools for submerged breakwaters.

Acknowledgments

The large-scale tests in the large wave channel (GWK) of the Coastal Research Centre FZK have been supported by European Community under the Access to Research Infrastructures Action of the Human Potential Programme (contract HPRI-CT-1999-00101). The authors thank Dr. J.H. Loveless (University of Bristol) for supplying the data. G. Festa and L. Gesuele are also acknowledged for their support in tests and data analysis.

Appendix A. Wave transformation across the front slope of a submerged breakwater

In deriving our model it has been assumed that if waves did not break onto the front slope of the breakwater, wave height at the outer edge of the structure crown equalled approximately the incident one. In principle, this means that wave shoaling on the breakwater face is negligible or, more precisely, that effects of shoaling and reflection somehow compensate each other. Using experimental data at our disposal, an effort has been directed to verify this hypothesis.

In some of *UoN* experiments (regular wave tests) a wave probe was mounted at the centre of the barrier crest; since the model was rather narrow ($B = 0.25$ m) results from this gauge have been assumed to be the same as at the beginning of the crest. To make the analysis more reliable only experiments where the waves were not seen to break have been considered. In GWK random wave experiments a wave probe was placed just at the beginning of the breakwater crest that is excellent for our scopes. Unfortunately, there were no tests in which waves did not break. To cope with this problem we employed only the breakwater models with a -0.4 submergence. This is because in those tests most of the waves broke on the crown, many of them landward the probe.

Results of the analysis are shown in Fig. A1, where the incident wave height (H_i) is compared with that at the breakwater crest (H_bc). Note that the zero up crossing significant wave height has been used as wave parameter, because it should better account non-linearity effects associated with the wave–structure interaction (Thompson and Vincent, 1985). Altogether experimental data seem to corroborate our hypothesis, at least on average; this apart from a couple of points belonging to *UoN* data (they are circled in Fig. A1I) where a surprising decay of wave height has been detected. This is possibly due to damping effects caused either by seepage or by a slight spilling not surveyed at naked eye. For *UoN* the ratio $H_{1/3\mathrm{bc}}/H_{1/3\mathrm{i}}$ (i.e. the shoaling ratio) varied between 0.71 and 1.35, with a 1.05 mean. Total 80% of points lay in the interval 0.9–1.2. As far as GWK random wave experiments are concerned the shoaling ratio resulted between 1.01 and 1.16, with a 1.06 mean. On the whole present results agree with findings of Gourlay (1994) who found, for a coral reef, the shoaling coefficients were included between 0.87 and 1.18 with a mean just over 1.0.

References

Basco, D.R., Yamashita, T., 1986. Towards a simple model of the wave transition region in the surf zone. In: Proceeding of the 20th International Conference on Coastal Engineering, ASCE, Taipei, pp. 955–970.

Bellotti, G., 2004. A simplified model of rip currents systems around discontinuous submerged barriers. Coastal Engineering 51, 323–335.

Buccino, M., Calabrese, M., 2007. Conceptual approach for the prediction of wave transmission at low crested breakwaters. Journal of Waterways, Port, Coastal and Ocean Engineering 133 (3).

Buhr-Hansen, J., 1990. Periodic waves in the surf-zone: analysis of experimental data. Coastal Engineering 14, 19–41.

Calabrese, M., Vicinanza, D., Buccino, M., 2002. Large scale experiments on the behaviour of low crested and submerged breakwaters in presence of broken waves. In: Proceedings of the International Conference on Coastal Engineering, ASCE, Cardiff, UK, pp. 1900–1912.

Calabrese, M., Vicinanza, D., Buccino, M., 2003. Wave set-up behind low crested breakwaters. In: Proceedings of the International Conference on Offshore end Polar Engineering, Honolulu, USA, May 2003.

Calabrese, M., Vicinanza, D., Buccino, M., 2005. Verification and re-calibration of an engineering method for predicting 2D wave setup behind submerged breakwaters. In: Proceedings of the 2nd International Coastal Symposium, Hoepn, Iceland, June 2005.

Calabrese, M., Pasanisi, F., Buccino, M., 2006. Sull'interazione tra moto ondoso e barriere sommerse (in Italian). In: Proceedings of the XXX Convegno Nazionale di Idraulica e Costruzioni Idrauliche, Rome, Italy, September 2006.

Cappietti, L., Clementi, E., Aminti, P., Lamberti, A., 2006. Piling up and filtration at low crested breakwaters of different permeability. In: Proceedings of the 30th International Conference on Coastal Engineering, ASCE, San Diego, USA, pp. 4957–4969.

Dalrymple, R.A., 1978. Rip currents and their causes. In: International Conference of Coastal Engineering, ASCE, Hamburg, pp. 1414–1427.

Dalrymple, R.A., Dean, R.G., 1971. Piling-up behind low and submerged permeable breakwaters. Discussion note on Diskin et al. (1970). Journal of Waterways and Harbors Division WW2, 423–427.

d'Angremond, K., van der Meer, J.W., de Jong, R.J., 1996. Wave transmission at low-crested structures. In: Proceedings of the International Conference of Coastal Engineering, ASCE, Houston, USA, pp. 2418–2426.

Daniel, P., 1952. On the limiting clapotis. Gravity waves: circular no. 521, National Bureau of Standards, pp. 35–38.

Dean, R.G., Chen, R., Browder, A.E., 1997. Full scale monitoring study of a submerged breakwater, Palm Beach, Florida, USA. Coastal Engineering 29.

Dick, T.M., 1968. On solid and permeable submerged breakwaters. CE Research Report No. 59, Queens University, Ontario.

Diskin, M.H., Vajda, M.L., Amir, I., 1970. Piling-up behind low and submerged permeable breakwaters. Journal of Waterways and Harbors Division WW2, 359–372.

Di Pace, P., 2006. Riflessione di onde regolari in presenza di opere a gettata (in Italian). Ph.D. Thesis, University of Naples Federico II.

Gourlay, M.R., 1971. Piling-up behind low and submerged permeable breakwaters. Discussion note on Diskin et al. (1970). Journal of Waterways and Harbors Division WW1, 219–222.

Gourlay, M.R., 1994. Wave transformation on a coral reef. Coastal Engineering 23, 17–42 (Elsevier).

Gourlay, M.R., 1996. Wave set-up on coral reefs. 1. Set-up and wave generated flow on an idealised two dimensional horizontal reef. Coastal Engineering 27, 161–193.

Grue, J., 1992. Nonlinear water waves at a submerged obstacle or bottom topography. Journal of Fluid Mechanics 244, 455–476.

Homma, M., Hoikawa, K., 1961. A study on submerged breakwaters. Coastal Engineering in Japan 4, 85–102.

Hattori, M., Sakai, H., 1994. Wave breaking over permeable submerged breakwaters. In: Proceedings of the International Conference of Coastal Engineering, ASCE, Kobe, Japan, pp. 1101–1114.

Homma, M., Sokou, T., 1959. An experimental study on the submerged breakwaters. Coastal Engineering in Japan 2, 103–109.

Hur, D.S., Kawashima, N., Iwata, K., 2003. Experimental study of the breaking limit of multidirectional random waves passing over an impermeable submerged breakwater. Ocean Engineering 30, 1923–1940.

Iwata, K., Kiyono, H., 1985. Breaking of standing two component composite and irregular waves. Coastal Engineering in Japan 28, 71–87 (Institution of Engineers, Australia, 2004).

Kamphuis, J.W., 1991. Incipient wave breaking. Coastal Engineering 15, 185–203.

Lamberti, A., 2005. Editorial paper on DELOS project. Coastal Engineering 52, 815–818 (Elsevier).

Lamberti, A., Martinelli, L., Zanuttigh, B., 2007. Prediction of wave induced water flow over and through the structure, of set-up and rip-currents. In: Environmental Design Guidelines for Low Crested Coastal Structures, Section 13.5. Elsevier, Amsterdam.

Lang, S., Ladson, T., Anderson, B., 2004. A review of empirical equations for estimating stream roughness and their application to four streams in Victoria. Australian Journal of Water Resources 8 (1), 69–82.

Longuet-Higgins, M.S., 1967. On the wave induced difference in mean sea level between two sides of a submerged breakwater. Journal of Marine Research 25, 148–153.

Longuet-Higgins, M.S., Stewart, R.W., 1962. Radiation stress and mass transport in gravity waves, with application to surf beats. Journal of Fluid Mechanics 13, 481–504.

Longuet-Higgins, M.S., Stewart, R.W., 1964. Radiation stress in water waves: a physical discussion with applications. Journal of Deep Sea Research 11, 529–563.

Loveless, J.H., Debski, D., 1997. The design and performance of submerged breakwaters. Report completed for UK Ministry of Agriculture, Fisheries and Food, Contract no. CSA 2606, University of Bristol, UK, p. 137.

Loveless, J.H., Debski, D., McLeod, A.B., 1998. Sea level set-up behind detached breakwaters.In: Proceedings of the International Conference on Coastal Engineering, ASCE.

Mansard, E.P., Funke, E.R., 1980. The measurement of incident and reflected spectra using a least squares method. In: Proceedings of the 17th Coastal Engineering Conference, ASCE, New York, pp. 154–172.

Nelson, R.C., 1996. Hydraulic roughness of coral reef platforms. Applied Ocean Research 18, 265–274.

Okayasu, A., 1989. Characteristics of turbulence structures and undertow in the surf zone. Ph.D. Dissertation, University of Tokyo.

Panizzo, A., Briganti, R., van der Meer, J.W., Franco, L., 2003. Analysis of wave transmission behind low-crested breakwaters using neural network. In: Proceedings of the Coastal Structures, Portland, USA, 2003.

Pasanisi, F., Buccino, M., Calabrese, M., 2006. Observation of breaker types at submerged breakwaters. In: Proceedings of the 2nd Short Course on Coastal and Port Engineering, Cosenza, Italy, May 2006.

Ranasinghe, R., Turner, I.L., 2006. Shoreline response to submerged structures: a review. Coastal Engineering 53, 65–79 (Elsevier).

Sawaragi, T., 1995. Coastal Engineering Waves, Beaches, Wave–Structure Interactions. Elsevier, Amsterdam.

Seji, M., Uda, T., Tanaka, S., 1987. Statistical study on the effect and stability of detached breakwaters. Coastal Engineering in Japan 30 (1), 131–141.

Svendsen, I.A., 1984. Mass flux and undertow in the surf zone. Coastal Engineering 8, 347–365.

Thompson, E.F., Vincent, C.L., 1985. Significant wave height for shallow water design. Journal of Waterways, Port, Coastal and Ocean Division., 828–842.

van der Meer, J.W., Briganti, R., Zanuttigh, B., Wang, B., 2005. Wave transmission and reflection at low-crested structures: design formulae, oblique wave attack and spectral change. Coastal Engineering 52 (10–11), 915–929.

Zanuttigh, B., van der Meer, J.W., 2006. Wave reflection from coastal structures. In: Proceedings of 30th International Conference on Coastal Engineering, vol. 5. ASCE, San Diego, USA, pp. 4337–4349.